2004

Understanding Mid-Latitude Space Weather: Storm Impacts Observed at BLO on 31 March 2001

Jan Josef Sojka
Utah State University

D. Rice

J. V. Eccles

F. T. Berkey

P. Kintner

W. Denig

Recommended Citation
Sojka, J. J., D. Rice, J. V. Eccles, F. T. Berkey, P. Kintner, and W. Denig (2004), Understanding midlatitude space weather: Storm impacts observed at Bear Lake Observatory on 31 March 2001, Space Weather, 2, S10006, doi:10.1029/2004SW000086.

Understanding midlatitude space weather: Storm impacts observed at Bear Lake Observatory on 31 March 2001

J. J. Sojka,[1] D. Rice,[2] J. V. Eccles,[2] F. T. Berkey,[3] P. Kintner,[4] and W. Denig[5]

Received 16 April 2004; revised 7 July 2004; accepted 2 August 2004; published 26 October 2004.

[1] On 30 March 2001 in the late evening an auroral display was observed over the United States of America. The Bear Lake Observatory (BLO) magnetometer in Utah measured changes of 550 nT in less than 30 min. During the same period, BLO ionosonde measurements showed deep high-frequency radio wave absorption up to 7 MHz. BLO's GPS single-frequency receiver experienced geolocation errors of 20 m for over 3 hours. These storm signatures were also accompanied by *L*-band scintillation effects which approached an S4 value of 0.2, which is large for midlatitudes. Although such measurements have been have been made at midlatitude locations for many decades, our knowledge of the processes and couplings involved in such events remains incomplete and, at best, qualitative. The interpretation of key ionospheric parameters' storm response is discussed in the context of present-day auroral and geospace electrodynamics understanding. We find that at BLO (L = 2.38) the available data raise more questions and can provide almost no answers without observational inputs from other locations. One solution to this impasse is to field a ground-based sensor network to resolve the spatial scales of the geospace electrodynamics. On the basis of the instrument complement at BLO, we argue for a contiguous U.S. deployment of modest magnetic/optical/RF observatories to observe the next solar maximum period's geomagnetic storms and to use these data to explore the physical processes and couplings on space weather effective scales in assimilative models in conjunction with space-based observations. *INDEX TERMS:* 2407 Ionosphere: Auroral ionosphere (2704); 2431 Ionosphere: Ionosphere/magnetosphere interactions (2736); 2788 Magnetospheric Physics: Storms and substorms; *KEYWORDS:* electrodynamics, assimilation, observations, ionosonde, magnetometer, GPS receiver

Citation: Sojka, J. J., D. Rice, J. V. Eccles, F. T. Berkey, P. Kintner, and W. Denig (2004), Understanding midlatitude space weather: Storm impacts observed at Bear Lake Observatory on 31 March 2001, *Space Weather*, *2*, S10006, doi:10.1029/2004SW000086.

1. Introduction

[2] For the past two decades, the relevance of large geomagnetic storms to terrestrial technology and humanity has developed practical significance. Two national programs have been created to address the scientific issues. The interagency National Space Weather Program (NSWP) attempts to qualify and forecast these effects. In contrast, the NASA Living with a Star (LWS) program aims at unraveling the mechanisms and phenomena from their source on the sun to their final terrestrial impact.

[3] From an operational standpoint, the Federal Aviation Administration (FAA) through its Wide Area Augmentation System (WAAS) deployments is quantifying the magnitude of one aspect of space weather, namely, the reliability of augmented single-frequency GPS geopositioning for aircraft (and other users) operating at midlatitudes.

[4] The WAAS system is perhaps the most open to the scrutiny of the space weather impacts and our knowledge of geomagnetic storms. It is being deployed over the United States of America as a set of more than 20 dual-frequency GPS receivers capable of locally determining the ionospheric corrections for single-frequency (1.575 GHz) GPS users. These corrections are assimilated in real time to produce improved corrections for single-frequency GPS users throughout the United States, such as the airline industry. The corrections are then transmitted via satellite to specially equipped GPS receivers, providing enhanced accuracy for geolocation and navigation. Operationally, the WAAS system is prone to its largest errors when the ionosphere is perturbed either in restricted regions, that is, localized high-density gradients, or by ionospheric structures (TIDs) traveling over the United States. Extensive scientific literature exists to quantify some of these geomagnetic storm effects. [*Buonsanto*, 1999, and references therein]. However, none of these observations or physical models contributes to the NSWP objective of specifying and forecasting space weather effects at levels that fulfill

[1]Center for Atmospheric and Space Sciences, Utah State University, Logan, Utah, USA.
[2]Space Environment Corporation, Providence, Utah, USA.
[3]Space Dynamics Laboratory, Utah State University, Logan, Utah, USA.
[4]Department of Electrical and Computer Engineering, Cornell University, Ithaca, New York, USA.
[5]Air Force Research Laboratory/Space Vehicle Directorate Battle Space Environment Division Center for Excellence in Space Weather, Space Plasma Disturbance and Forecasting Sections, Hanscom Air Force Base, Massachusetts, USA.

any systems goals. Present-day knowledge of the physical processes at their effective operating spatial and temporal scales can best be viewed as "climatology."

[5] Aside from the GPS system, geomagnetic storm impacts on other technologies and society in general are not yet fully understood despite decades of study. High-frequency (HF) radio communications are particularly susceptible to disruption from storm-related absorption and scintillation effects. Communication links at frequencies below about 100 MHz may fail as the storm-modified ionospheric critical frequencies (f_OE, f_OF2) change, causing the maximum useable frequency (MUF) to shift abruptly; failures may be due to loss of the channel when the MUF drops, or to interference from distant signals that are received when the MUF increases. Geolocation systems other than GPS such as over-the-horizon (OTH) radars have enhanced and undetermined errors caused by excessive ionospheric parameter fluctuation.

[6] During the most intense phases of these storms when strong *D*-region absorption occurs, the existence of very energetic particles is inferred from the enhanced ionization of this lower region of the ionosphere. The energy range and fluxes of these particles are poorly understood and hence their impact upon satellites, space shuttles, the International Space Station and the humans on board are all uncertain, as is the question of how low into the atmosphere the particles penetrate. At middle and equatorial latitudes, that is, equatorward of the auroral regions, conventional wisdom holds that Low Earth Orbit (LEO) satellites are outside of the regions of energetic auroral precipitation, but this assumption fails in disturbed times!

[7] The issue of geomagnetically induced currents (GIC) at midlatitudes is similarly unquantified. At high latitudes, GIC effects on power grids and pipelines are well known [see, e.g., *Pirjola*, 2000] and protective measures may be taken; the consequences of not taking adequate precautions are well documented [*Kappenman and Albertson*, 1990]. However, the effects at midlatitudes are largely unstudied and the importance of GIC precautions are less clear to the power industry, so the potential for power grid disruptions related to geomagnetic storms (and storm sudden commencements in particular [*Kappenman*, 2003]) remains.

[8] In Sections 2 through 6 of this paper, a set of midlatitude observations of space weather is presented, and in Section 7 they are discussed from a chronological point of view in the context of the NSWP and a geomagnetic storm. This leads to a suggestion on how a step function in our knowledge can be achieved. Section 8 summarizes how this advance may be achieved. The term *geomagnetic storm* means different things to different people and as such it is an overarching qualitative term with little or no physics being implied. Hence in Sections 2 through 6, observations from BLO will be presented as the empirical record of a specific geomagnetic storm at that location. However, in Section 7, this empirical information will be discussed in the more specific context of physical processes and of our best present-day efforts to understand the inner workings of a geomagnetic storm.

2. BLO and the Storm of 31 March 2001

[9] The Bear Lake Observatory (BLO) located at 41.94°N and 248.59°E is operated jointly by the Space Dynamics Laboratory (SDL) and the Center for Atmospheric and Space Sciences (CASS) at Utah State University. The observatory is located in a rural environment on the western shores of Bear Lake in northern Utah. At the time of the 31 March 2001 geomagnetic storm, the observatory was making ionospheric measurements with an ionosonde, an all-sky imager, a pair of fluxgate magnetometers and an *L*-band scintillation receiver. One of the magnetometers and the L-band scintillation receiver were fielded at BLO by Space Environment Corporation (SEC). In terms of the geomagnetic location, BLO is at an L of 2.38 and has a corrected geomagnetic latitude of 49.6°; it would normally be viewed as a midlatitude station under plasmaspheric field lines.

[10] The major geomagnetic storm on 31 March 2001 was successfully forecasted by NOAA. Indeed, the lead author used the NOAA storm forecast given during the local television news broadcast at 10:00 p.m. 30 March MST (0500 31 March UT) as motivation to observe the impending aurora beginning around 11:00 p.m. MST (0600 UT). This storm was classical in temporal profile though its magnitude was unusually large. The *Dst* index (Figure 1) was close to zero for 12 hours prior to its main phase (up to 0500 UT on 31 March 2001), then rapidly decreased to its storm minimum of −358 nT in only 5 hours. The storm *Dst* then recovered over a 3-day period. During the initial 5 hours and for the first day of recovery, the planetary *Kp* index remained above 5 (Figure 1). At the peak of the storm, two successive 3-hourly *Kp* values were 9−. These values are very large given the *Kp* scale is pseudologarithmic and has a maximum value of 9. Since 1957, there have only been 7 geomagnetic storms whose *Dst* index was more negative than −350 nT and 47 geomagnetic storms in which the planetary *Kp* index equaled or exceeded 9^-. This justifies viewing the 31 March 2001 event as a major geomagnetic storm.

[11] The source of the geomagnetic storm on 31 March 2001 is associated with the solar wind, which at almost exactly 0000 UT on 31 March 2001 underwent major changes in the vicinity of the Earth. Figure 2 shows the ACE satellite observation of the Interplanetary Magnetic Field (IMF) and plasma for a 3-day period referenced to 0000 UT on 31 March 2001. Solar wind conditions prior to the storm, from −24 to 0 hours in Figure 2, are very quiescent. However, on 31 March huge departures from the prior day occurred in the IMF as well as in solar wind speed, temperature and density. Only the solar wind density showed significant activity prior to 0000 UT on 31 March with densities increasing from undisturbed values of 10 cm^{-3} to 30 cm^{-3} at 2100 UT on 30 March.

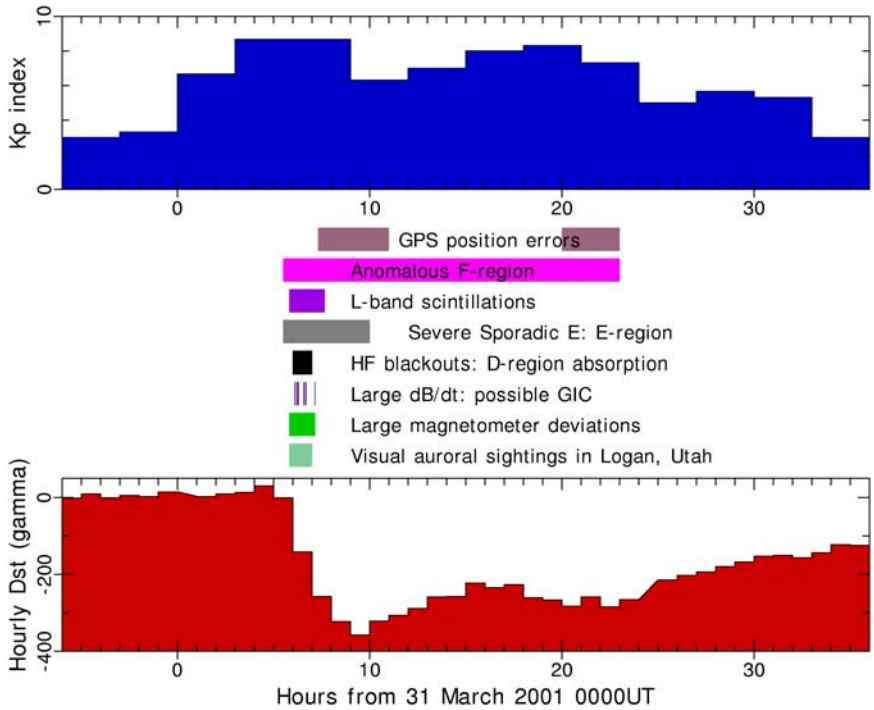

Figure 1. Chronology of space weather observations at BLO/Logan on 31 March 2001 in the context of the planetary geomagnetic *Kp* and *Dst* indices.

[12] From 0000 UT on 31 March, the solar wind is highly disturbed for about 24 hours. However, during the period of disturbances observed at BLO, 0600 to 0730 UT on 31 March, the solar wind is relatively quiescent; this one and a half hour period is emphasized in the right-hand panels of Figure 2. Note that conventionally the propagation time required for the solar wind to travel from the ACE satellite to the magnetopause, about 35 min for a solar wind speed of 700 km/s, would be used to shift the ACE observations to the magnetospheric reference frame. For this study, this time shift has not been introduced since the solar wind data are presented only as an indication of the complexity of the solar wind. However, the 35 min offset makes the solar wind density drop observed by ACE at about 0530 UT coincide with the 0600 UT activity observed at BLO; did that change cause the auroral breakup over northern Utah?

[13] Anecdotally, the observing conditions were ideal for auroral observations. Unfortunately, the all-sky camera system operating at BLO was making low light level measurements of midlatitude airglow. The auroral intensities were so large that this optical instrument was saturated during the auroral activity.

3. BLO Magnetic Record

[14] Figure 3 shows the magnetic field record and inferred horizontal field variation from 0400 UT to 0900 UT on 31 March 2001. These times are offset by 7 hours from the BLO Mountain Standard Time (MST). Hence the peak BLO deviation occurred at 0620 31 March UT corresponding to 11:20 p.m. on 30 March MST when the auroral displays were also approaching their most dynamic phase. The most significant aspect of Figure 3 is the rapidity and magnitude of the magnetic field variations which were caused by currents flowing in the ionosphere. The magnetometer axes are positioned such that X is magnetic north, Z is toward the center of the earth, and Y completes the right-hand coordinate system (eastward). All three components showed comparable deviations: X component from 18,761 to 19,670 nT; Y component from 4,073 to 4,573 nT; and Z component from 49,231 to 49,878 nT. These correspond to 909, 500 and 647 nT changes for the X, Y, and Z components over the same 40-min period from 0600 to 0640 UT. For context, a major auroral substorm would be associated with a ''negative bay'' magnetic deviation of up to 1000 nT in the H component of auroral magnetometers and almost no deviation at midlatitudes. Figure 3 (bottom panel), shows the variation in the H component that readily exceeds 500 nT over a 30-min interval.

[15] The magnetic temporal signature observed at BLO is consistent with the presence of an electrojet flowing in the ionosphere. However, to reduce these one-station magnetic records to the spatial and temporal record of the current systems is not unique. The major deviation seen as a positive deviation on each component between 0607 and 0625 UT occurred when the local auroral observers saw the main development of auroral arc-ray brightening associated with both equatorward expansion over BLO (and Logan) and east to west expansion of the most dynamic auroral forms. During this period, the X compo-

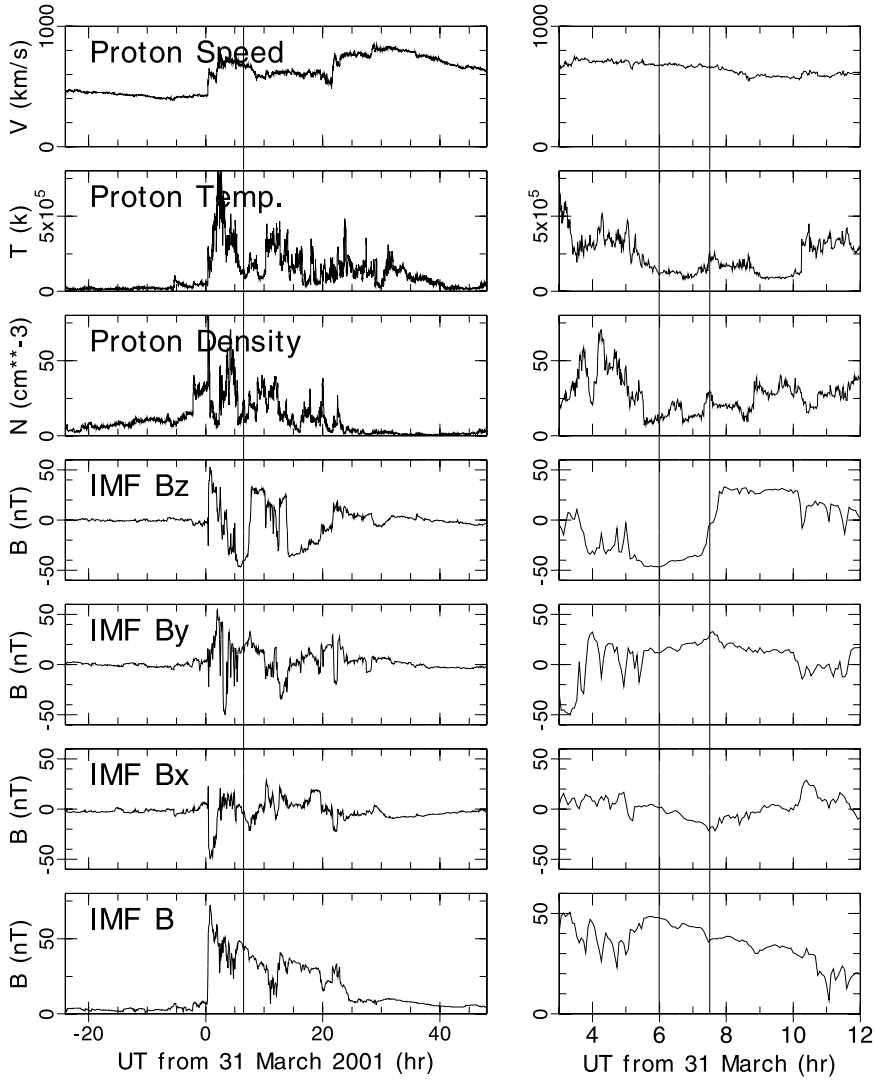

Figure 2. ACE satellite solar wind observations for 30 March through 1 April 2001. The panels represent (top to bottom) proton speed, proton temperature, proton density, interplanetary magnetic field (IMF) B_z, IMF B_y, IMF B_x, and magnetic field strength. A vertical line at 0600 UT represents the time of interest for the BLO storm observation. The right-hand series of panels expands this time period, showing the solar wind parameters from 0300 to 1200 UT with two vertical lines representing the interval of disturbances at BLO.

nent increased by 500 nT, the Y component by 250 nT, and the Z component by 200 to 250 nT (relative to a decreasing *Dst* storm background). In addition, all three components show deviations with similar timescales. These three component variations are best described by an overhead current flowing to the southeast. At its peak, this oversimplified current would be required to be 200–300 kA if overhead at 100 km altitude and assuming induced ground currents increased the observed magnetic field by 3/2, following the calculation of a simple equivalent current given by *Hargreaves* [1992, pp. 193–194].

[16] These ionospheric current systems are not quasi-static, but in addition to the electrojet motion described above, have high-frequency components. These rapid variations make them geoeffective in terms of ground induction effects, that is, geomagnetically induced currents (GIC). In this case, it is the time rate of change of the magnetic field that is important; that is, the X component (Figure 3) shows a 500 nT spike that rises and falls in 20 min which yields sustained dB/dt values of 0.42 nT/sec. Over shorter time periods, the dB/dt values are as large as 6.1, 6.8, and 6.1 nT/s respectively in the X, Y, and Z components. Observations at higher latitudes in Finland have shown that dX/dt values of 6–8 nT/s induce GIC of about 40 A in 400 kV power lines [*Viljanen*, 1998]. *Kappenman* [2003] has presented a study of how storm sudden commencement events are a source of GIC at low latitudes and midlatitudes. Our BLO study, though not specifically at the

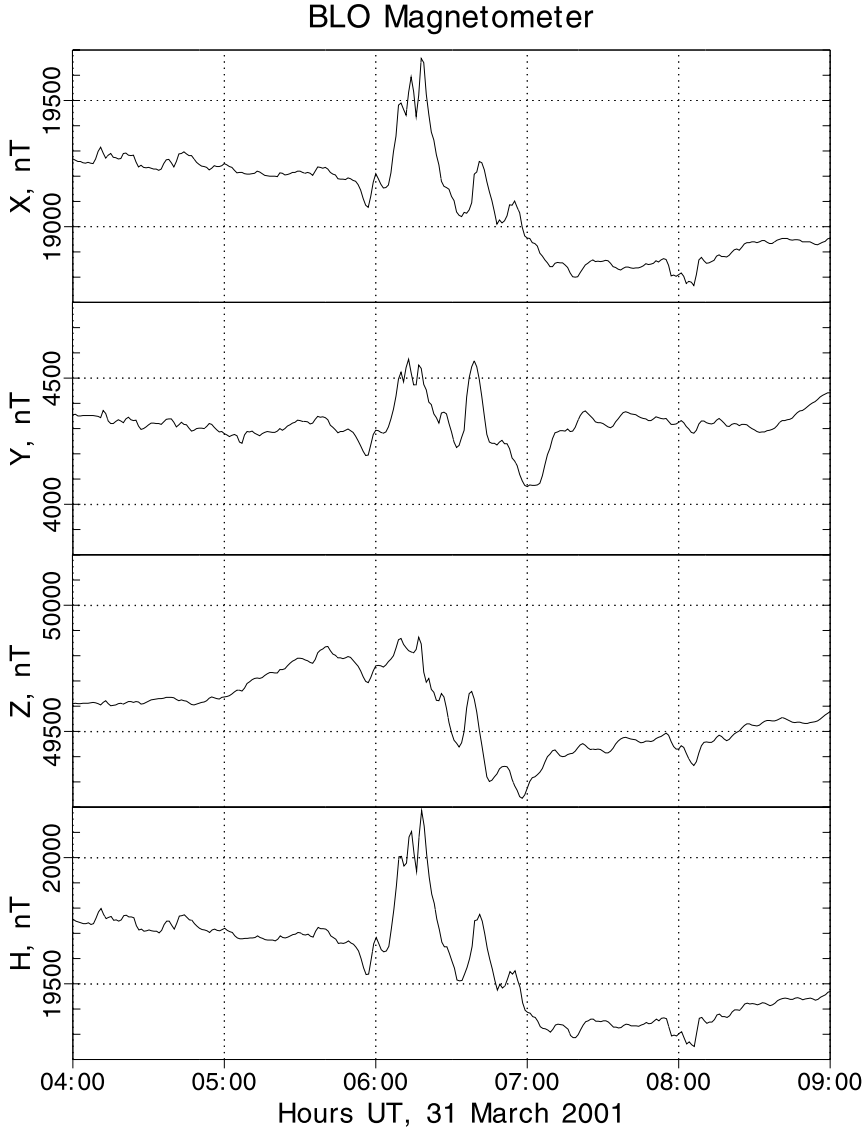

Figure 3. BLO magnetometer magnetic field components and (bottom) horizontal magnetic field from 0400 to 0900 UT on 31 March 2001.

sudden commencement of the storm, does appear to have similar midlatitude attributes.

[17] In the context of space weather specification and forecasting, these electrodynamics signatures resulting from intense ionospheric currents are a) not contained in any present-day empirical model, b) beyond present-day physical modeling capabilities, and c) extremely localized in both space and time within the global picture of a geomagnetic storm. The recent modeling work of *Ridley and Liemohn* [2002] attempts to create partial ring currents self-consistently which, in turn, would be associated with structured electrodynamics at midlatitudes in the ionosphere. Observationally, *Wygant et al.* [1998] using electric field measurements from the CRRES spacecraft showed how structured and intense these midlatitude electrodynamics become in a geomagnetic storm. Hence even though BLO captured the local variability and strength of the midlatitude electrodynamics, our knowledge of the processes is not sufficient to describe how the electrodynamics evolved.

4. BLO Ionosonde Observation

[18] The geomagnetic storm of 31 March 2001 produced an auroral latitude–like response in the ionosphere above BLO, affecting the ionosphere down to *D*-region heights where significant absorption occurred, as manifested by marked changes in f_{min}. Although *D*-region absorption effects are sometimes present during daytime as a result of solar X-ray events or anomalous midlatitude winter absorption, no similar nighttime absorption has previously been measured at BLO. An overview of the temporal

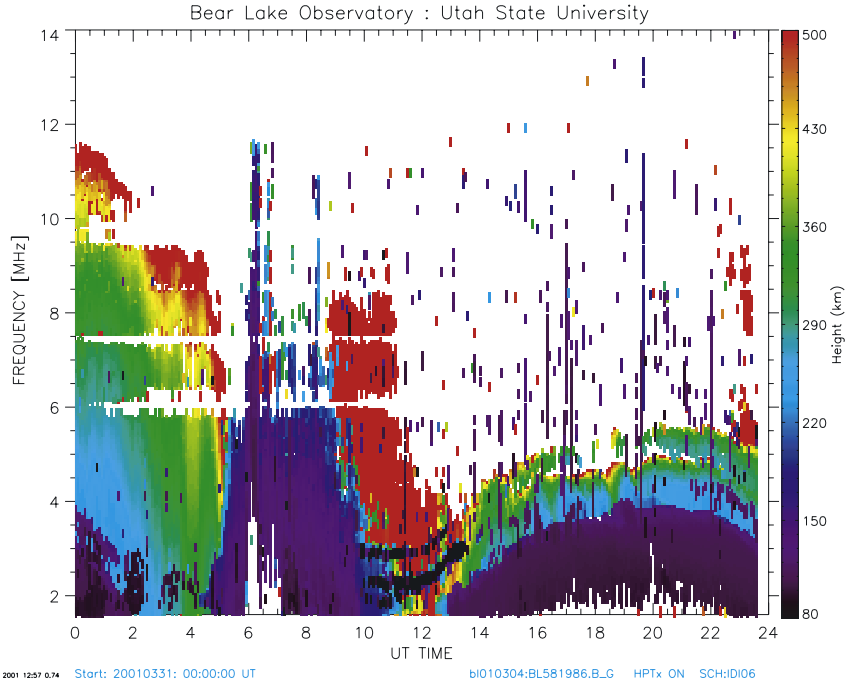

Figure 4. BLO dynasonde observations of the ionosphere from 0000 to 2400 UT on 31 March 2001. The individual ionograms are vertical color-coded lines in which color represents virtual height (km) and the vertical axis is the sounding frequency (MHz).

variation in the local ionosphere on 31 March 2001 is illustrated in Figure 4, which displays frequency as a function of time using color to denote the virtual height of reflection within each individual ionogram. The UT day is thereby represented by 288 columns comprising ionograms acquired at 5-min intervals. In Figure 4, the color varies from black (80 km) to red (500 km); multiple-hop *F* region echoes are generally not depicted. Between 0555 and 0710 UT, these data show increased f_{min} implying that intense *D*-region precipitation occurred over this interval. The ionogram data show that this precipitation varied from sounding to sounding, with f_{min} varying between 2.3 and 4.7 MHz at 0605 UT. For much of the time after the storm onset, intense sporadic *E* dominated the ionogram measurements, the top frequency of which was 12 MHz during the nighttime period. Clearly, the ionosphere was rapidly changing during this interval with considerable "spread" appearing in both the *E* and *F* regions; particularly noteworthy is the appearance of dense (to 8 MHz) spread *F* ionization at altitudes in excess of 500 km between 0840 and 1110 UT. Since the upper limit of dynasonde range gate sampling is at 750 km, no information above that height is available, although the presence of *F*-region structure above that height can be inferred from ionograms. Between 1000 and 1330 UT, two distinct black traces appear on the ionogram (Figure 4) separated by 0.7 MHz in the 2 to 3.5 MHz range. These are caused by range aliasing of O and X echoes from above 750 km. At high latitudes, ionogram "blackout" is generally associated with this type of geomagnetic storm, so the ionospheric variations detected by the USU dynasonde, although very chaotic, are somewhat unique in that the ionospheric echoes were not totally absorbed by the *D*-region ionization.

[19] Additional confirmation of this midlatitude high-energy precipitation comes from the Defense Meteorological Satellite Program (DMSP) observations (not shown here). On 31 March 2001, four DMSP satellites made measurements of these auroral particles, namely: F12, F13, F14, and F15. Unfortunately, during the key 0600 to 0700 UT period, all four satellites made auroral passes in the southern hemisphere. DMSP F15 between 0620 and 0623UT was crossing strong auroral precipitation in the southern hemisphere in the 2300 MLT sector at magnetic latitudes between 46° and 54°. This sector is magnetically conjugate to BLO to within about 30 min of magnetic local time (MLT). Both ion and electron precipitation spectra have significant fluxes at 10 keV with peak precipitation at about 1 keV for electrons and a few keV for ions. The equatorward edge of these fluxes is at about 46° magnetic latitude, which is equatorward of BLO in the conjugate hemisphere. These electrons are the source of the observed auroral structures. Over the same latitude range, the DMSP F15 in situ plasma drift and magnetometer instruments also observed significant departures. The horizontal plasma drift was maintained at over 1 km/s from 48° to 53° magnetic latitude and was associated with an upward vertical plasma drift of 0.7 km/s. Assuming that these same plasma drifts mapped to the conjugate northern hemisphere region, then the 0.7 km/s upward drift would readily account for the very high *F*-region echoes observed by the dynasonde at BLO.

[20] Although these ionospheric observations show common geomagnetic storm effects from a space weather point of view, even their specification is challenging. The intense absorption effects observed between 0600 and 0700 UT are associated with the intense electrodynamics discussed in Section 3. Hence the present-day ability to specify or forecast this absorption with any quantitative accuracy is nonexistent. The effects on the nighttime *F* layer, 0600 to 1300 UT, are longer lasting and involve storm "positive" and "negative" phases which probably have a greater coherence scale than the current systems. Most certainly, this is the case for the subsequent reduced daytime *F* layer from 1300–2400 UT in Figure 4. *Basu et al.* [2001a] show almost the identical ionospheric storm response from a digisonde located at Westford, Massachusetts on 22 October 1999; see Figure 11 of *Basu et al.* [2001a]. The review paper by *Buonsanto* [1999] extensively describes these midlatitude ionospheric storm responses. However, given that the ionospheric storm drivers, the magnetosphere and the thermosphere, have quite different spatial and temporal characteristics and source regions, the accurate modeling of the ionospheric storm is beyond the present-day capabilities of either statistical or physical ionospheric models. It may well be possible, though, with assimilation models currently under development.

5. BLO *L*-Band Scintillation Observations

[21] The GPS system operates in the UHF L band at two frequencies 1.2276 and 1.57542 GHz. Standard GPS position determination units that cost less than $1,000 (the hand-held variety) are all single-frequency systems. SEC was monitoring the quality of single-frequency *L*-band GPS signals at BLO during the storm in question using a single-frequency system developed by Dr. Paul Kintner and his research team at Cornell University. This unit not only monitors positioning information but also scintillation on each satellite link. At any given time between 4 and 12 GPS satellites can be observed. From these links, an evaluation of the quality of the L-band radio frequency (RF) reception can be made. The unique attribute of this GPS receiver system is that it automatically samples the L1 frequency at 50 Hz and is able to calculate the S4 scintillation index for each GPS satellite link as

$$S4 = \frac{\sqrt{\overline{P^2} - \left(\overline{P}\right)^2}}{\overline{P}} \quad (1)$$

where P is the sampled signal power. This scintillation detection technique is described by *Ledvina et al.* [2002]. Ledvina et al. studied GPS scintillations observed at Cornell University, Ithaca, New York, on the 26 September 2001. They found extremely large-amplitude scintillations reaching S4 values of 0.8 associated with the equatorward edge of the midlatitude trough in the sunset local time sector. Their observation provides yet another example of the challenges provided by extreme space weather effects to present-day modeling. At this time, the only mature scintillation model is the Wideband Model (WBMOD,) which is a statistical model of scintillation occurrence probabilities [*Secan et al.*, 1995, 1997]. For a phenomenon as poorly understood as the global or local occurrence of irregularities that lead to scintillations, the ability to specify and possibly forecast midlatitude scintillations will require a real-time observational approach, that is, assimilation modeling.

[22] Figure 5 provides the BLO scintillation record from 0400 to 0900 UT on 31 March 2001. In Figure 5, the solid line represents the average value of S4 while the upper and lower dashed lines represent the maximum and minimum S4 values, respectively. The scintillation is measured via the S4 index and during this time almost reaches 0.2. More importantly, all GPS satellites observed show S4 values in excess of 0.05 during the 0615 to 0635 UT period. Under normal conditions, the S4 index at BLO would range from 0 to 0.03. This spread is attributed to satellites at lower elevation being prone to multipathing problems that can provide S4 index contamination. Single satellites at very low elevation angles, less than 25°, can cause spurious S4 values through multipathing, but these effects can readily be identified and have been removed.

[23] Figure 5 shows that the S4 values observed at BLO are spread over a range. Reduction of each separate GPS satellite link to determine a latitude and longitude of the ionospheric L-band ray pierce points shows that the strongest scintillations were observed toward the northeast of BLO. Hence although the BLO signals showed no GPS dropouts, this may have been fortuitous in that no GPS satellite line of sight went through a particularly severe irregularity region in the ionosphere.

[24] The presence of measurable L-band scintillation at midlatitudes probably indicates very severe scintillation was present at VHF and lower UHF. *Basu et al.* [2001a, 2001b] provide detailed examples of this L band to lower UHF/VHF difference in the S4 intensity over the low-latitude to midlatitude region during geomagnetic storms. However, the low-latitude mechanisms associated with the dusk sector Rayleigh-Taylor instability is quite different from the midlatitude mechanism which is, in this case, associated with an auroral electrojet that has expanded to midlatitudes from high latitudes. This electrojet association of the midlatitude S4 enhancement (Figure 5) can be seen by correlating it with the BLO H component storm variations in Figure 3 (bottom panel). As a result, the specification and forecast of this space weather effect is as poor as that for the current (electrodynamics) discussed in Section 3. This midlatitude auroral electrojet scintillation is also a different source mechanism than that associated with the intense midlatitude scintillations observed by *Ledvina et al.* [2002].

6. BLO GPS Position Variability

[25] Clearly, the GPS receiver at BLO is fixed at a given location. However, since single-frequency operation of a GPS unit is unable to compensate fully for the ionosphere,

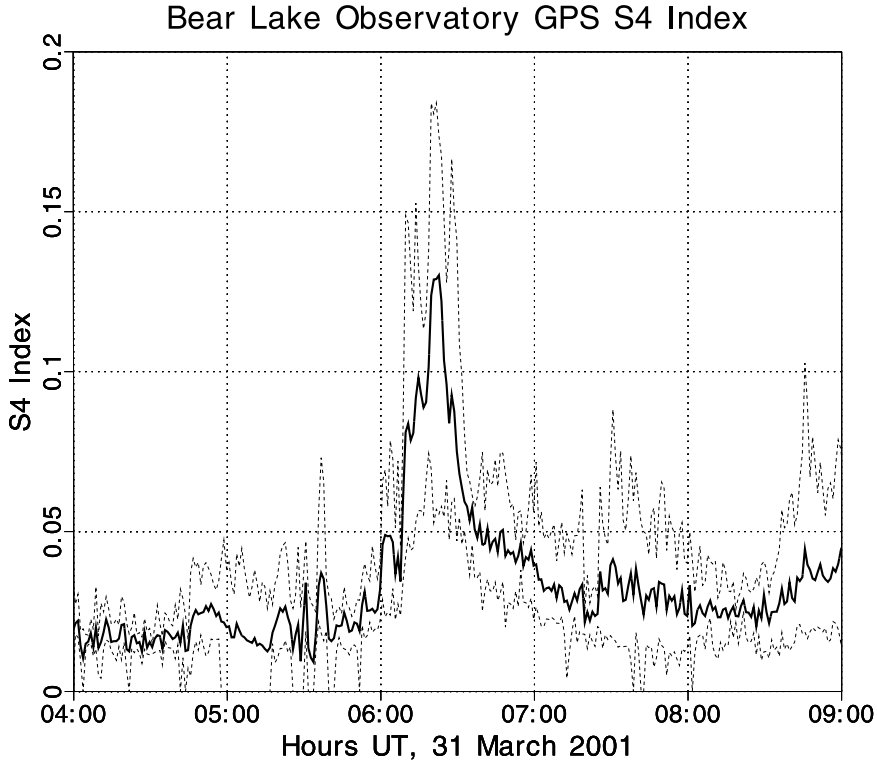

Figure 5. BLO GPS receiver average S4 index (solid line), smallest S4 value (lower dashed line), and largest S4 value (upper dashed line) from 0400 to 0900 UT on 31 March 2001.

significant errors in the station location measurement do occur. SEC has used this receiver to monitor the magnitude and dynamics of the positioning errors. Figure 6 shows the BLO position latitude, longitude, and altitude errors over the 0400 to 1200 UT period on 31 March 2001. The bottom panel in Figure 6 shows absolute position error at BLO. This time range has been extended from that used in Figures 3 and 5 because the GPS position errors are not synchronized with either the magnetic disturbance or scintillation levels but depend upon the ionospheric density variability. In each panel the solid trace represents the 31 March values while the dashed line represents the median position error over the previous six days. During this 8-hour interval there were no large systematic errors, often caused by poor GPS satellite geometries and which tend to occur at the same time each sidereal day for several days.

[26] All three position error components show a coherent, although not synchronized, time variation of the position error from 0700 to 1100 UT, a period of 4 hours that begins an hour after the main BLO auroral, magnetic, and scintillation activity. The latitude and altitude errors are most significant. The latitude error ranges from −10 m to +10 m while the altitude error ranges from more than −10 m to +20 m. From 25 to 30 March 2001, the BLO position error had a standard deviation of 5.0 m in latitude, 3.4 m in longitude, and 8.2 m in altitude. The 4 hour period of latitude and altitude errors as large as two standard deviations is an ionospheric storm effect.

[27] A second major excursion of BLO GPS occurred during this storm. From 2000 to 2300 UT on 31 March 2001, the overall errors reached 20 m and were sustained for several hours (Figure 7). This later period, beginning 14 hours after the storm began at BLO, occurs in the late afternoon sector prior to 1800 LT. In contrast, the auroral storm features described previously were seen prior to midnight at 2300 LT. During the late afternoon, *Foster et al.* [2000, 2002] and *Basu et al.* [2001a] have reported considerable ionospheric density structuring during storms. Specifically, they have used ground-based GPS TEC instruments to identify a general depletion of plasma over the United States with a superimposed ridge of plasma which is oriented from Florida in a north to northwest direction across the United States. This structure initially runs along the east coast of the United States and over a period of hours turns to a more northwesterly orientation. The structure is stable for hours, and Foster et al. have associated its presence with the subauroral polarization stream (SAPS) electric field structures. Fortuitously, *Foster et al.* [2002] have studied the 31 March 2001 period and their Figure 2 shows a snapshot of the GPS TEC over the United States at 1930 UT on 31 March 2001. Much of the midwestern and western United States has TEC values between 10 and 50 TECu, while the east coast in the vicinity of the high-density structure has TEC values well over 100 TECu.

[28] Assuming that this structure turns northwest a few hours later and sweeps over BLO, it would give rise to a

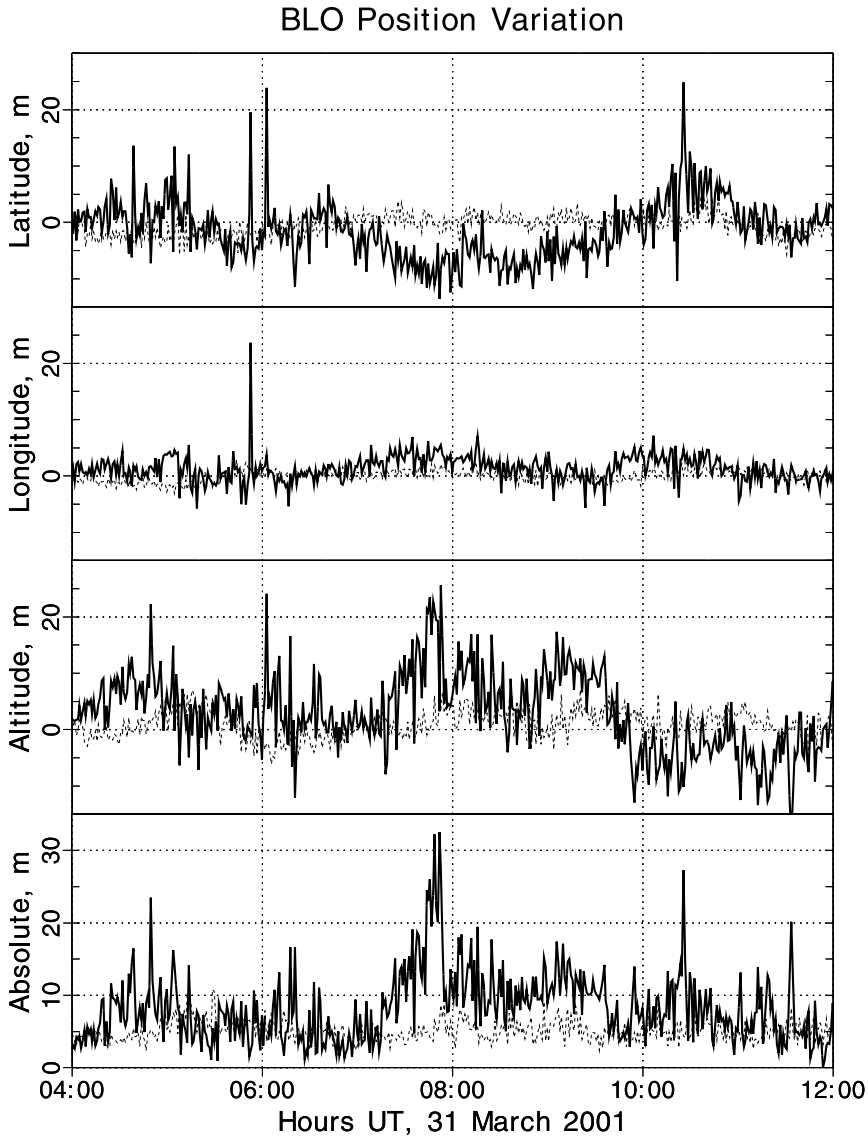

Figure 6. BLO GPS single-frequency geolocation coordinate errors and (bottom) absolute error from 0400 to 1200 UT on 31 March 2001 (solid line) compared with the median value of the previous 6 days (dashed line).

TEC gradient passing over BLO with the low-density side being close to 10 TECu while the higher-density side would be above 100 TECu. In all probability, these gradients in the ionospheric *F* layer are responsible for much of the enhanced error in positioning seen in Figure 7. This error arises because different BLO receiver-to-GPS satellite link paths traverse quite different TEC which, in turn, cause the L1 receiver algorithms to make erroneous calculations. For the worst case example at 2120 UT, the total BLO position error reached 30 m (Figure 7, bottom panel). To map this into a TEC value requires a knowledge of the satellite geometry and hence an estimation of the geometric dilution of precision (GDOP) factor. For typical GDOP values in the range 2–3, the 30 m uncertainty yields a TEC of 94–62 TECu. These values of TEC and TEC gradients are readily within the range of values reported by *Foster et al.* [2002] on this particular afternoon. However, it is unlikely that such a sustained TEC feature had formed 14 hours earlier at local midnight to produce the large GPS position errors recorded at BLO (Figure 6) an hour after the local auroral storm commencement.

7. Discussion

[29] The geomagnetic storm on 31 March 2001 beginning at 0500 UT occurred at an optimal time to create a variety of space weather effects in the three major layers of the ionosphere in the American longitude sector. Table 1 lists these effects as recorded at the Bear Lake Observatory in Utah. From a space weather viewpoint, all of these effects

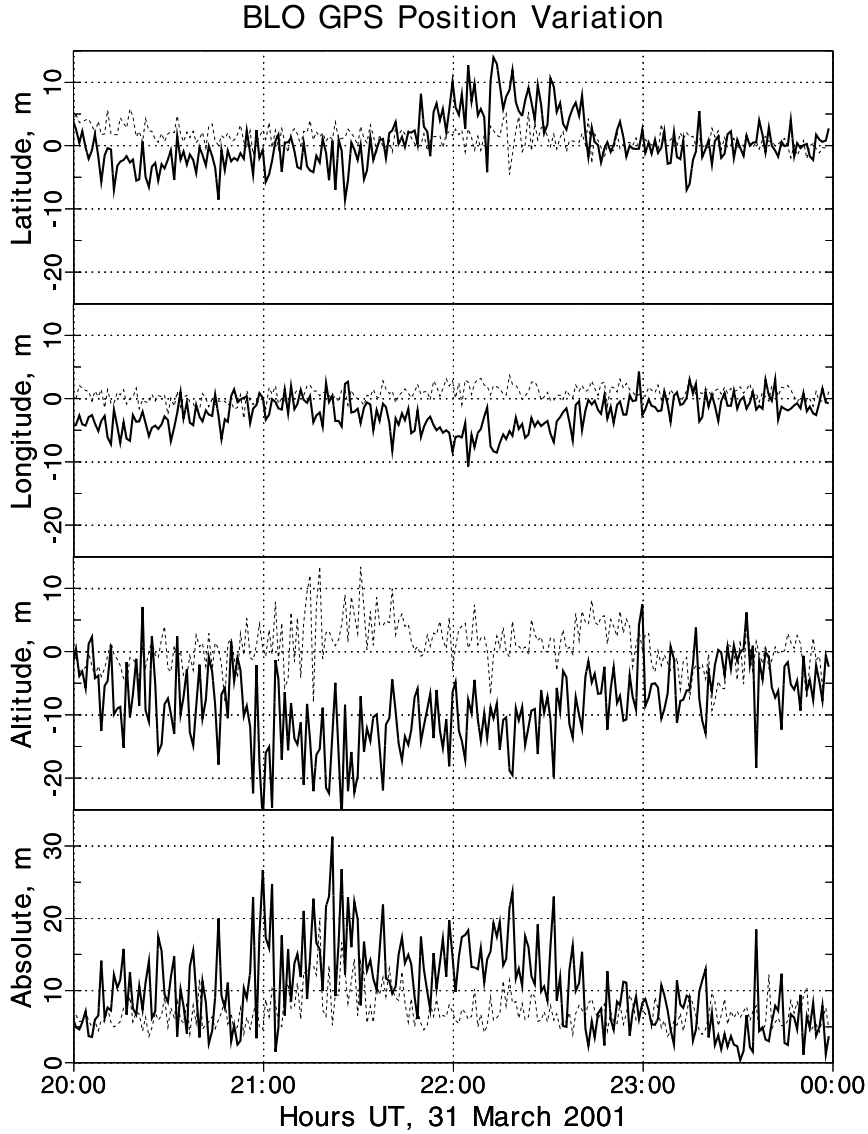

Figure 7. BLO GPS single-frequency geolocation coordinate errors and (bottom) absolute error from 2000 to 2400 UT on 31 March 2001 (solid line) compared with the median value of the previous 6 days (dashed line).

occurred during a major geomagnetic storm. However, from a specification or forecast perspective, these phenomena are relatively asynchronous and of different duration within the geomagnetic storm time line. Figure 1 attempts to organize the Table 1 space weather events chronologically relative to the *Dst* and *Kp* indices which describe the global characteristics of the geomagnetic storm. Possibly the most evident result of this organization is that the space weather effects observed at BLO have their peak between 0600 and 0700 UT, which is unrelated to any specific feature in the global indices or in the solar wind (Figure 2). The duration of the intense electrodynamic effects is less than an hour and all appear somewhere during the 5-hour main phase of the storm. Other locations would experience their local storm effects at different times, with higher-latitude regions probably experiencing them earlier in the main phase as the auroral boundaries move equatorward. However, to specify the time and duration of these effects at each location is beyond the capability of present-day empirical or physical modeling.

[30] Some insights into the difficulties of understanding the storm effects can be obtained by applying present-day understanding of the geospace processes to the specific observations listed in Table 1 and Figure 1. The observation of auroral arcs, their ''blue green'' colors, and their east-to-west alignment and development all confirm that ''energized'' precipitating electrons were responsible. DMSP observations of such electrons in the conjugate hemisphere support this contention, and indicate that their energies were a few to tens of keV. A more interest-

Table 1. Logan/Bear Lake Observatory Space Weather on 31 March 2001

Space Weather Effect	Duration, UT	Impact	Major Cause
Visual auroral display	0550–0700	"Beautiful"	Particle precipitation
Magnetometer **B** deviation	0550–0710	**B** deviations	Ionospheric currents
Large *dB*/*dt*	Events between 0615–0710	GIC	Temporal changes in current
HF blackouts	0600–0700	No propagation of HF <4 MHz	*D*-region ionization by very high energy particles
D- and *E-region* absorption	0530–1000	Absorption of HF waves	*D*- and *E*-region ionization by high-energy particles
L-band scintillation[a]	0550–0740	Signal loss of lock	Auroral instability mechanisms
Anomalous *F* region	0530–2300	HF coordinate registration errors	Various
GPS L1 position errors	0720–1100, 2000–2300	Errors >3 m	Various

[a]Although no measurements were made at VHF or lower UHF, scintillation at these frequencies would have to be severe and of longer duration.

ing reflection is the question: where did they come from? The auroral display was observed for 30+ min at L = 2.38 and reported even further equatorward. A conventional geospace interpretation of auroral arcs places the most equatorward arc near the inner edge of a plasma sheet; was this located at 2.38 R_e in the equatorial plane? Following the same conventional geospace interpretation, were the storm time ring currents equatorward of 2.38 R_e? This places all of the regions inside the Van Allen radiation belts. Given that the radiation belts survive relatively unmodified through decades of geomagnetic storms, do they require maintenance of a magnetic flux tube topology inconsistent with conventional ideas of how ring currents, inner edge and plasma sheet field lines develop to produce auroral magnetic field lines and auroral electrodynamics? The auroral observations imply field-aligned precipitation; did the electrons get energized on route from a plasma sheet reservoir to the ionosphere? If so, the 2,000 to 10,000 volts of acceleration normally associated with auroral inverted V precipitation would be restricted to a rather short length of an L = 2.38-type field line. This case would require extremely large field aligned electric potentials: a worst case scenario would involve 2,000 to 10,000 volts over 10,000 km!

[31] The second observation listed in Table 1 is the ground-based magnetometer readings and inferred geospace currents that closed in the ionosphere above BLO. These observations are not explained by a simple equatorward shift of the standard auroral westward electrojet. As inferred from the magnetic records in Section 3, the current system was not an eastward system; however, the magnitude of the inferred current and even its time rate of change are in the range of geoeffective auroral events. From a geospace understanding these dynamic nonstandard current systems would be described as part of an asymmetric ring current system. However this in fact does not carry with it any useful specification or forecast information. These local currents are evidence that indeed the L = 2.38 field line was an integral part of a geospace magnetosphere-ionosphere (M-I) current system which is often viewed as a region 1–2 current system that links the outer magnetosphere through the ionosphere with closure through the ring currents. If in this case the evening sector region 1 is at L = 2.38 or equatorward, does this imply the ring current closure is even further equatorward?

[32] Perhaps a more difficult issue for space weather specification and modeling is that during these storm growth phases, lasting up to half a day, the standard concept of the midlatitude and low-latitude ionospheres being shielded from high-latitude magnetospheric electrodynamics does not apply. At the L = 2.38 location for about 30 min, extremely large M-I current variations were observed that imply similar variability in electric fields. The standard model of M-I coupling argues that the ring currents adjust to the high-latitude electric fields with a time constant of about 30 min and shield the lower latitudes. Given that the ring currents are themselves moving in at least latitude, their role in shielding a dynamic driver seems unlikely. Once again this phenomenon falls under the asymmetric ring concept that at the present time is only an argumentative set of processes.

[33] The next two items from Table 1, HF blackouts and *D-E* region absorption, are rarely discussed in the context of geospace electrodynamics. However, these effects are temporally correlated with the electrodynamics, and the enhanced *D*-region ionization producing absorption implies energetic particles significantly more energetic than a few to 10 keV. These considerations link the observations into the physics. At the L = 2.38 location, the magnetic field lines are not only associated with an auroral energization mechanism, a plasma sheet–type source, and a ring current, but also pass through the radiation belts. In standard auroral models this latter population is not present. Most auroral models do not address the presence of *D*-region ionization and its associated HF blackouts. The questions of which particle source is responsible for the *D*-region ionization and how the storm time electrodynamics cause the precipitation at these low L values are unanswered.

[34] The observation of severe L-band scintillation during the period of strong current flows is perhaps readily associated with the standard auroral field-aligned current models in which field-aligned currents that exceed threshold values lead to current instabilities and these in turn lead to local ionospheric plasma irregularities. The impact of these irregularities is to cause scintillation of radio

Table 2. Western U.S. Magnetometer Observations on 31 March 2001

Location	Geographic Latitude, °N	Geographic Longitude, °E	Distance to BLO, km	Magnetic Latitude, °N	Magnetic Longitude, °E
Newport, Wash.	48.27	242.88	834	55.14	304.5
BLO, Utah	41.94	248.59	0	49.60	313.1
Boulder, Colo.	40.14	254.76	554	48.78	320.6
Tucson, Ariz.	32.17	249.27	1088	40.23	316.1

waves traversing these regions. Hence the observation of scintillations could be interpreted as evidence of auroral field-aligned currents exceeding current instability thresholds on L = 2.38 magnetic field lines.

[35] The final two items listed in Table 1, *F*-region anomalies and GPS position errors, are consequences of an ionosphere highly disturbed by energy inputs over many hours. These energy inputs are associated with both direct storm effects and delayed effects presumed to be from the thermosphere, which has slower response times. Some energy may be tied to the inner magnetosphere via the SAPS phenomenon. In any case, these ionospheric effects are very relevant to space weather but are not temporally or spatially correlated with the prior discussion of storm-related geospace electrodynamics.

[36] The BLO suite of observations thus describes the temporal evolution of the physical processes, if only at one location. Combined with similar observations from other ground locations or satellite observations, such data would in principle provide maps of both the temporal and spatial evolution of the processes. These maps would in turn provide information defining the physical processes' scale sizes and hence the scale of the model needed to understand them, that is, global scale, macroscale (thousands of km,) mesoscale (hundreds of km,) or microscale (<100 km). At this time, our observations of these large storms indicates that a wide range of observables (Table 1) are modified significantly and many vary on timescales of seconds, while others are on hour to day timescales. In the mapping sense, the evidence is less clear about the spatial scale of the phenomena. Anecdotal information from reports of auroral sightings indicates that the storm of 31 March 2001 was seen across the United States, implying a continental scale for the visual phenomena.

[37] Figure 2 of *Foster et al.* [2002] showed that later on 31 March 2001 the ionospheric density as measured by the integrated electron content was reduced over much of North America, indicating an ionospheric storm negative phase, but over the east coast at 1930 UT an extended north-south enhanced density structure existed. This structure has macroscales in north-south extent and mesoscales in the east-west direction. *Saito et al.* [1998] studied ionospheric structures, specifically traveling ionospheric disturbances (TIDs) using over 900 GPS receivers distributed over Japan. This particular distribution of GPS sensors had an average spacing of 25 km and found TIDs with typical wavelengths of 300 km [see *Saito et al.*, 1998, Figure 3]. The 300 km wavelength is comparable to the density/TEC gradient scale sizes reported by *Foster et al.* [2002]; hence a GPS distribution less dense than that used by Saito et al. would be adequate to follow the storm evolution in the ionosphere. In fact, the present-day distribution of ground-based GPS receivers may already be adequate.

[38] The U.S. Geological Survey (USGS) fields several magnetometers across the United States. The three nearest BLO are listed in Table 2. Boulder is on the same L shell, 554 km east of BLO, while Tucson is almost due south by 1088 km, and Newport is 834 km northwest. Figure 8 shows the H component magnetic field from these three stations along with that of BLO. Boulder and BLO are well correlated, being at the same L value, in sharp contrast to the H component dynamics seen at Tucson and Newport. One may thus be tempted to argue that in the east-west direction one is dealing with a macroscale problem, while in the north-south direction the phenomenon is mesoscale or finer.

[39] The limitation for magnetic signature mapping compared to GPS TEC mapping is that we do not have sufficient magnetic observations to show coherent features; GPS TEC observations have a sufficient distribution of instruments to show considerable spatial detail. This discrepancy is unfortunate, since the magnetic signature provides information on the ionospheric current systems and hence on the electrodynamics that drive the M-I system. In contrast, the TEC maps provide information on the ionosphere's response (electron density structures) following other M-I storm responses, and these are not simply cause-and-effect relationships. As discussed earlier, on the basis of Table 1 and Figure 1, it is reasonable to consider the SAPS-driven north-south ionospheric structures in the TEC maps as having a different driver than the storm time, predominantly east-west aligned phenomena seen at BLO from 0600–0730 UT.

[40] Similar problems of scale and driver mechanism arise when trying to understand the enhanced HF absorption observed at midlatitudes. The ionogram sequences portrayed in Figure 4 show nighttime absorption during the peak of the electrodynamic disturbances which would be caused at that time by energetic particle precipitation, producing *D*- and *E*-region ionization. Given that this absorption is associated with the electrodynamics, it would be modeled on a macroscale east-west and on a microscale north-south. However, at midlatitudes it is well known that daytime HF absorption events occur [*Thomas*, 1961] which last from hours to a few days. These events have been found to have macroscale structures [*Schwentek*, 1974]. The mechanism for this latter midlatitude absorption effect is unclear, but tends to follow storms, is strongest during winter, and is probably associated with the storm production and transport of [NO]. Again, the prob-

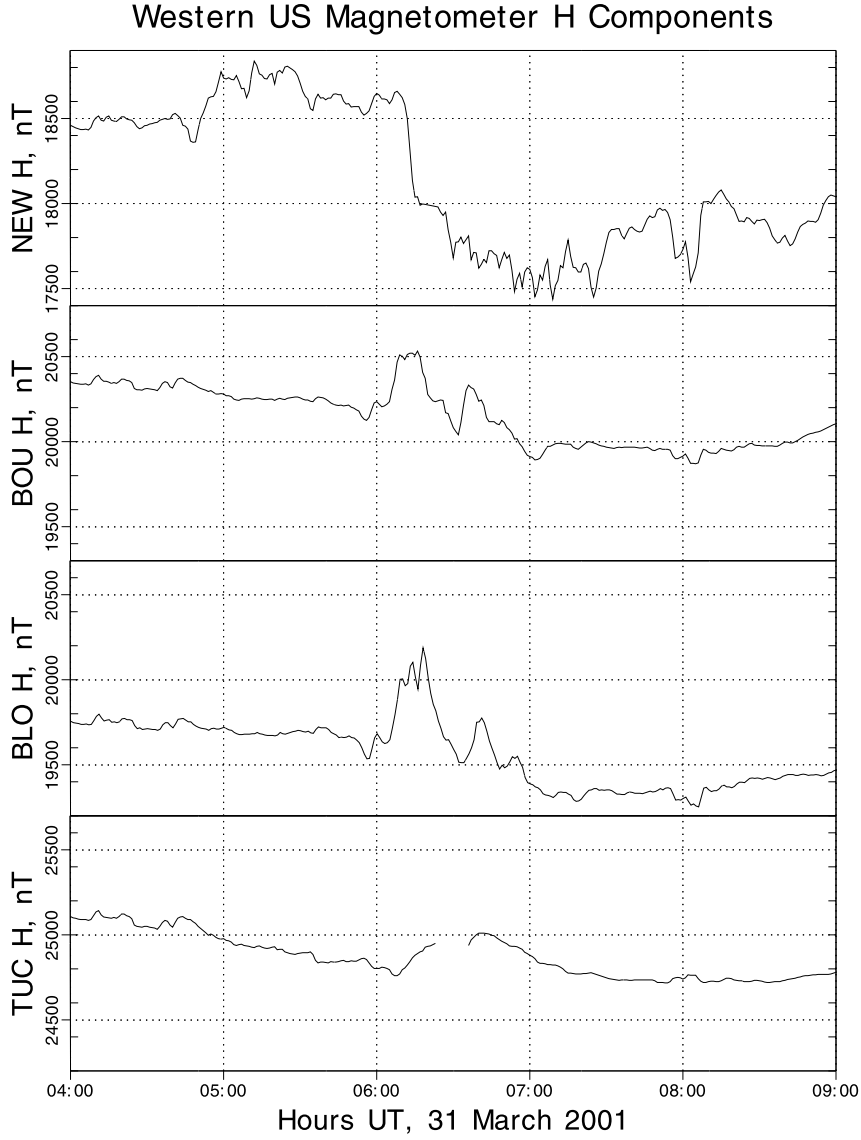

Figure 8. Western U.S. magnetometer observations from 0400 to 0900 UT on 31 March 2001.

lem is that both forms of HF absorption are observed but neither has been mapped sufficiently to elucidate their source mechanisms.

[41] How are these questions to be addressed?

[42] A systems approach using satellites and ground-based sensors that drive or are assimilated into models to test our physical knowledge of the system or to provide specification and forecast for space weather application is advocated by the Decadal Survey report [*National Research Council*, 2002]. Neither the present-day satellite nor ground-based sensor distributions are able to provide the needed observations, with the exception of the GPS TEC network. Figure 9 is a map of the "readily available" observations provided by CEDAR and NGDC/SPIDR for recent years; sites shown in Figure 9 are listed in Table 3 and data may be found through http://cedarweb.hao.ucar.edu/ and http://spidr.ngdc.noaa.gov/spidr/. Clearly, there are only a few magnetometers, ionosondes, and optical instruments available from these resources. Of course, the databases are not exhaustive; some BLO instruments do not appear in either the NGDC/SPIDR or CEDAR registries. Even so, there are clearly too few measurements to address the meso/macroscale problems of the storm.

[43] The Decadal Survey addresses such problems by suggesting the deployment of a distribution of small sensors to operate in real time and as a network. This concept has been further explored by a National Academy of Sciences Committee of Solar and Space Physics workshop (8–9 May 2004) to study a Distributed Array of Small Instruments (DASI).

[44] For the large geomagnetic storm that is the topic of this study, the DASI concept would be on a meso/macroscale and hence could be tackled by a U.S. network.

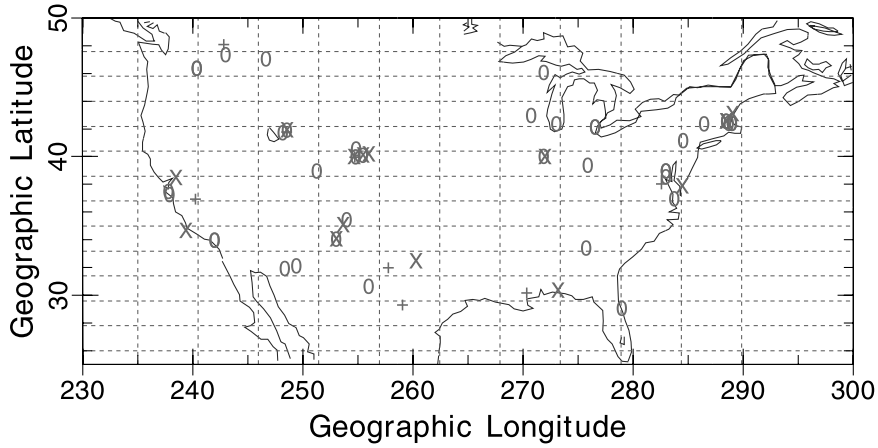

Figure 9. Magnetic (pluses), optical (0s), and ionosonde/radar (crosses) observations for the contiguous United States available from CEDAR and NGDC/SPIDR databases for this decade. Stations that discontinued contributing to these databases prior to 2002 have been omitted.

During the dynamic "auroral" phases of the storm, the east-west scales appear to be longer than the north-south scale, suggesting a distribution more compact in latitude than longitude. Superimposed on Figure 9 are latitude-longitude grid lines with 500 km longitude spacing and 200 km latitude spacing. Over the United States, this grid has 102 cells and represents a DASI whose longitude scale tends toward macro scale, while its latitude scale captures mesoscales. The BLO instrumentation provides a starting place to address the question of what each "small instrument" suite might be. Table 1 identifies the physical parameters/process and the associated instrument/measurement. Missing from this suite are optical measurements and measurements of plasma drift electrodynamics. Overall, our experience with the complement of instruments at BLO leads us to believe that the small instrument suite needs to contain magnetic, optical and RF (MORF) measurement techniques to capture the range of processes at play.

[45] A network of such small instruments would consist of passive instruments (P-MORF observatory) augmented with strategically placed active instruments (A-MORF observatory). BLO represents a mixture of active and passive instruments, which is occasionally problematic in a small observatory because of mutual interference. The MORF observatory would be entirely automated, requiring only a small instrument enclosure and sufficient real estate to set up sensors and antennas. A P-MORF observatory might consist of:

[46] • Magnetometer

[47] • Optical: all-sky imager and/or Fabrey-Perot interferometer

[48] • RF: GPS TEC/scintillation monitor, riometer, oblique sounder receiver, and/or HF monitor

[49] An A-MORF observatory could include instruments such as lidars, meteor radars, HF beacons, and low-power sounders. The active instruments might preclude the use of some passive instruments, depending on the real estate available to separate any sensors subject to mutual interference. A-MORF observatories would be significantly more expensive to build and operate than P-MORF observatories, and would have more impact on their neighbors, so their deployment would be somewhat limited.

[50] A hypothetical MORF sensor network deployed across the contiguous United States would serve three purposes:

[51] 1. Continuous observation of routine weather in the midlatitude ionosphere, allowing impacts of geomagnetic variations, X-ray flares, anomalous absorption, sporadic *E*, TIDs, etc. to be quantified for researchers, MF and HF communication engineers, and power utility engineers.

[52] 2. Observation of the effects of unusual, large-magnitude space weather phenomena such as the 31 March 2001 storm, allowing researchers to formulate and test theories that address these events, and possibly providing warnings to communications and power utility engineers.

[53] 3. Production of a consistent, reliable wide-area data stream for assimilative specification and forecasting models of the sort sought after by the NSWP.

Deploying a MORF sensor network would be a logical extension of the successful GPS TEC networks that now exist in the United States and elsewhere around the world, and should allow our understanding of mesospheric and ionospheric weather to evolve to a level comparable to that which currently exists for tropospheric weather — understanding that is largely due to the successful integration of meteorological models, space-based observations, and a large network of ground-based observations.

8. Conclusion

[54] The BLO measurements present an asynchronous set of midlatitude space weather observations during the 31 March 2002 geomagnetic storm. These observations and the magnitude of these space weather effects are not unique. During the recent solar maximum, many obser-

Table 3. Magnetic (M), Optical (O), and Radio Frequency Observations in the Contiguous United States Since 2000[a]

Location	M	O	RF	Geographic North Latitude	Geographic East Longitude	Magnetic North Latitude	Magnetic East Longitude
Aerospace Corp.		P[b]		34.0	242.0	41.2	308.3
Albany		P		42.4	286.5	53.2	358.8
Albuquerque			A[b]	35.1	253.7	43.8	321.0
Arizona, Univ. of		P[b]		32.2	249.4	40.4	316.8
Bear Lake Observatory	P	P	A, P	41.9	248.6	49.9	313.6
Berkeley		P		37.5	237.8	44.0	302.9
Boulder	P	P	A	40.1	254.8	48.9	321.1
Colorado State Univ.		A		40.6	254.9	49.4	321.1
Daytona Beach		P[b]		29.1	279.0	39.8	350.4
Del Rio	P			29.5	259.1	38.8	328.0
Durham			A	43.1	289.1	53.9	2.0
Dyess AFB			A	32.5	260.3	41.9	328.8
Eglin AFB			A	30.4	273.2	40.8	343.7
Fredericksburg	P			38.2	282.6	48.9	354.2
Fresno	P			37.1	240.3	44.0	305.7
Georgia Tech.		A		33.4	275.8	43.9	346.5
Goddard		P[b]		39.0	283.0	49.7	354.6
Glade Park		P[b]		39.0	251.3	47.4	317.4
Greeley			A	40.2	256.0	49.1	322.5
Hanscom AFB/AFGL		A, P	A	42.6	288.5	53.4	1.3
Illinois, Univ. of		P[b]		40.1	271.9	50.4	341.2
Iron Mountain		P		46.1	271.9	56.4	340.4
Kitt Peak		P		32.0	248.4	40.1	315.7
Langley		A		37.0	283.8	47.8	355.7
Lockheed		P		37.3	237.9	43.8	303.0
Los Alamos		P[b]		35.5	254.0	44.2	321.2
McDonald Observatory		P		30.7	256.0	39.7	324.3
Madison		P		43.0	270.8	53.2	339.5
Maryland, Univ. of		A[b]		39.0	283.0	49.7	354.6
Michigan, Univ. of		P		42.2	276.6	52.7	346.7
Millstone Hill		P	A	71.5	288.5	82.3	2.5
Naval Res. Lab.		P[b]		38.6	283.0	49.3	354.7
Newport	P			48.3	242.9	55.3	304.9
Peach Mountain		P		42.4	273.1	52.8	342.4
Pittsburgh, Univ. of		P[b]		41.2	284.6	52.0	356.5
Platteville		P	A	40.1	255.5	49.0	321.9
Point Arguello			A	34.7	239.4	41.4	305.3
Rattlesnake Mt./Richland		P		46.4	240.4	53.1	302.9
Sacramento			A	38.5	238.5	45.0	303.3
Seeley Lake		P		47.1	246.7	54.7	309.7
Socorro		P	A[b]	34.1	253.1	42.7	320.5
Stennis Space Cent.	P			30.4	270.4	40.6	340.5
Stewart Radiance Lab.		P[b]		42.6	288.5	53.4	1.3
Table Mountain		A		34.0	242.0	41.2	308.3
Tucson	P			32.2	249.3	40.4	316.7
Urbana			A	40.0	272.0	50.3	341.4
Utah State Univ.		A		41.7	248.2	49.6	313.2
Wallops Island			A	37.9	284.5	48.7	356.5
Whitworth College		P[b]		47.4	243.0	54.4	305.4
Wright Patterson AFB		A		39.4	275.9	49.9	346.1

[a]Instruments are classified as active (A) or passive (P). Magnetic coordinates are calculated for 1 July 2004.
[b]Instrument is mobile and may not be located at the listed site. Some sites (e.g., Boulder) host many instruments belonging to different organizations; coordinates should be taken as representative of the general vicinity.

vations on this scale have been reported, especially those associated with the extensively analyzed "Bastille Day Storm" of 15 July 2001. Individually, each observation has been repeated for more than four decades. Unfortunately, insight into the processes and physical couplings that create a geomagnetic storm is only advancing incrementally! Present-day knowledge is unable to quantify a geomagnetic storm and its adverse effects for NSWP specification or forecast needs.

[55] Each measurement made at BLO provides information about a specific process that occurs in geospace during the geomagnetic storm. The measurements listed in Table 1 are complementary, but as discussed above, they do not provide sufficient input to improve knowledge of geospace models. A conclusion from these discussions is that an extended set of such measurements would in fact provide answers to specific questions that would in turn advance our geospace knowledge. If the measurements were made over a grid stretching east to west and north to south across the contiguous United States, then the questions about the temporal and spatial scales of the geospace electrodynamics, their correlation scales, and how the

phenomena evolve across the continent could be answered. On the basis of available observations, we have suggested a grid size of 500 km by 200 km in longitude and latitude respectively. We believe that such an experiment would generate a surge of new knowledge, comparable to that produced by the International Geophysical Year (IGY), about geospace electrodynamics during times of particular interest to space weather researchers. Whether used to advance physical understanding of geospace or assimilated into models that specify or forecast geospace, these observations would open the door to better understanding the geomagnetic storm dynamics.

[56] Using this type of DASI data network will in itself pose new challenges for scientists and engineers. These data streams need to be combined into maps of the parameters, preferably in near–real time. In the first instance, having maps of the evolution of the phenomena (the M-I drivers and ionospheric responses) will provide a clear distinction between scale sizes and between physical mechanisms, as well as providing a monitoring capability for NSWP forecasters. Theoretically, these combined data sets will also challenge present-day ring current, partial ring current, radiation belt, and other inner magnetosphere-ionosphere storm evolution models. The observations will for the first time provide constraints and boundary conditions for how rapidly the processes evolve and migrate. The maps will also form a framework into which satellite observations can be placed and thus their temporal and spatial attributes can be resolved.

[57] The assimilation of these data, not as maps but as individual data streams, into physics-based models will not only lead to specification over the continent, but will also identify missing physics in the models, providing improved understanding of the physics and of the limitations in the computational implementations.

[58] The present-day lack of models to describe the M-I coupling during these events demonstrates the need for the theory-modeling community to develop such models that will assimilate these observations. In fact, the deployment of a DASI would only be the first part of a modern IGY-style effort to resolve storm physics.

[59] **Acknowledgments.** J. J. S. was supported by National Science Foundation grant ATM-0000171 and NASA grant NAG5-8227 to Utah State University, and F. T. B was supported by National Science Foundation grant ATM-0218206 to Utah State University. Space Environment Corporation work was supported by US Air Force SBIR contract F19628-00-0026. The GPS research at Cornell University was supported by ONR grant number N00014-92-J-1822. We thank the ACE MAG and SWEPAM instrument team and the ACE Science Center for providing the ACE data. We are grateful to NGDC/SPIDR for providing the USGS magnetometer data presented here.

References

Basu, S., et al. (2001a), Ionospheric effects of major magnetic storms during the international space weather period of September and October 1999: GPS observations, VHF/UHF scintillations, and in situ density structures at middle and equatorial latitudes, *J. Geophys. Res.*, *106*(A12), 30,389.

Basu, S., S. Basu, K. M. Groves, H.-C. Yeh, S.-Y. Su, F. J. Rich, P. J. Sultan, and M. J. Keskinen (2001b), Response of the equatorial ionosphere in the South Atlantic region to the great magnetic storm of July 15, 2000, *Geophys. Res. Lett.*, *28*(18), 3577, doi:10.1029/2001GL013259.

Buonsanto, M. (1999), Ionospheric storms: A review, *Space Sci. Rev.*, *61*, 193.

Foster, J. C., S. Basu, S. Basu, A. J. Coster, and F. J. Rich (2000), Sub-auroral ionospheric disturbances and space weather effects during the July 15–16, 2000 geomagnetic storm, *Eos Trans. AGU*, *81*(48), Fall Meet. Suppl., Abstract SH62A-10.

Foster, J. C., P. J. Erickson, A. J. Coster, J. Goldstein, and F. J. Rich (2002), Ionospheric signatures of plasmaspheric tails, *Geophys. Res. Lett.*, *29*(13), 1623, doi:10.1029/2002GL015067.

Hargreaves, J. K. (1992), *The Solar Terrestrial Environment*, Cambridge Univ. Press, New York.

Kappenman, J. G. (2003), Storm sudden commencement events and the associated geomagnetically induced current risks to ground-based systems at low-latitude and midlatitude locations, *Space Weather*, *1*(3), 1016, doi:10.1029/2003SW000009.

Kappenman, J. G., and V. D. Albertson (1990), Bracing for the geomagnetic storms, *IEEE Spectrum*, *27*, 27.

Ledvina, B. M., J. J. Makela, and P. M. Kintner (2002), First observations of intense GPSL1 amplitude scintillations at midlatitudes, *Geophys. Res. Lett.*, *29*(4), 1659, doi:10.1029/2002GL014770.

National Research Council (2002), *The Sun to the Earth and Beyond: A Decadal Research Strategy in Solar and Space Physics: Executive Summary*, Natl. Acad., Washington, D. C.

Pirjola, R. (2000), Geomagnetically induced currents during magnetic storms, *IEEE Trans. Plasma Sci.*, *28*, 1867.

Ridley, A. J., and M. W. Liemohn (2002), A model-derived storm time asymmetric ring current driven electric field description, *J. Geophys. Res.*, *107*(A8), 1151, doi:10.1029/2001JA000051.

Saito, A., S. Fukao, and S. Miyazaki (1998), High resolution mapping of TEC perturbations with the GSI GPS network over Japan, *Geophys. Res. Lett.*, *25*, 3079.

Schwentek, H. (1974), Some results obtained from the European Cooperation concerning studies of the winter anomaly in ionospheric absorption, in *Methods of Measurement and Results of Lower Ionosphere Structure*, edited by K. Rawer, p. 293, Akademie, Berlin.

Secan, J. A., R. M. Bussey, E. J. Fremouw, and S. Basu (1995), An improved model of equatorial scintillation, *Radio Sci.*, *30*, 607.

Secan, J. A., R. M. Bussey, E. J. Fremouw, and S. Basu (1997), High-latitude upgrade to the wideband ionospheric scintillation model, *Radio Sci.*, *32*, 1567.

Thomas, L. (1961), The winter anomaly in ionospheric absorption, *J. Atmos. Terr. Phys.*, *23*, 301.

Viljanen, A. (1998), Relation of geomagnetically induced currents and local geomagnetic variations, *IEEE Trans. Power Delivery*, *13*, 1285.

Wygant, J., D. Rowland, H. J. Singer, M. Temerin, F. Mozer, and M. K. Hudson (1998), Experimental evidence on the role of the large spatial scale electric field in creating the ring current, *J. Geophys. Res.*, *103*, 29,527.

F. T. Berkey, Space Dynamics Laboratory, Utah State University, Logan, UT 84322, USA.

W. Denig, AFRL/VSBXP, 29 Randolph Road, Hanscom AFB, MA 0173-3010, USA.

J. V. Eccles and D. Rice, Space Environment Corporation, 221 N. Spring Creek Parkway, Providence, UT 84332, USA.

P. Kintner, Department of Electrical and Computer Engineering, Cornell University, Ithaca, NY 14853, USA.

J. J. Sojka, Center for Atmospheric and Space Sciences, Utah State University, Logan, UT 84322-4405, USA. (fasojka@sojka.cass.usu.edu)